

## Supporting Information

# Photoinduced Magnetic Phase Transition and Remarkable Enhancement of Magnetization for a Photochromic Single-Molecule Magnet

Li-Zhen Cai, Pei-Yu Guo, Ming-Sheng Wang,\* and Guo-Cong Guo\*

State Key Laboratory of Structural Chemistry, Fujian Institute of Research on the Structure of Matter, Chinese Academy of Sciences, Fuzhou, Fujian 350002, P. R. China.

E-mails: gcguo@fjirsm.ac.cn, mswang@fjirsm.ac.cn

### Index:

1. Experimental Section .....	S2
1.1 Materials and Instruments .....	S2
1.2 Synthesis of $[\text{Dy}^{\text{III}}(18\text{C}6)(\text{H}_2\text{O})_3]\text{Fe}^{\text{III}}(\text{CN})_6 \cdot 2\text{H}_2\text{O}$ (DyFe18C6) .....	S2
1.3 Orang samples for magnetic studies .....	S3
1.4 X-ray crystallographic study .....	S3
2. Graphics .....	S5
3. Tables .....	S10

# 1. Experimental Section

## 1.1 Materials and Instruments

All chemicals were of reagent grade quality and purchased from commercial sources. A PLSSXE300C 300 W xenon lamp system equipped with an IR filter was used to prepare irradiated samples for PXRD, FT-IR, UV-vis, and ESR, studies, and a Newport Co. Pulseo GKNQL-355-3-30 diode pumped solid state (DPSS) laser (355 nm; 70 kHz; 39 ns pulse width; ca. 1.55 mJ/cm<sup>2</sup>; spot size, ca. 1.5 cm $\phi$ ) for magnetic susceptibilities studies. Elemental analyses of C, H, and N were performed on an Elementar Vario EL III microanalyzer. PXRD patterns were collected on a Rigaku MiniFlex II diffractometer using Cu  $K_{\alpha}$  radiation ( $\lambda = 1.5406 \text{ \AA}$ ). The simulated PXRD patterns were derived from the Mercury Version 2.3 software. FT-IR spectra were obtained on a Perkin-Elmer Spectrum One FT-IR spectrometer using KCl pellets in the range of 2300–450 cm<sup>-1</sup>. UV-Vis spectra were measured at room temperature on a Perkin-Elmer Lambda 900 UV/vis/NIR spectrophotometer with an integrating sphere attachment and BaSO<sub>4</sub> as a reference. ESR spectra were recorded on a Bruker ER-420 spectrometer with a 100 kHz magnetic field in the X band at room temperature. Magnetic measurement was carried out on a Quantum Design PPMS-9 superconducting quantum interference device (SQUID) magnetometer, and diamagnetic corrections were made using Pascal's constants.

## 1.2 Synthesis of [Dy<sup>III</sup>(18C6)(H<sub>2</sub>O)<sub>3</sub>]Fe<sup>III</sup>(CN)<sub>6</sub>·2H<sub>2</sub>O (DyFe18C6)

The reaction mixture of DyCl<sub>3</sub>·6H<sub>2</sub>O (0.377 g, 1 mmol), K<sub>3</sub>Fe(CN)<sub>6</sub> (0.012 g, 0.3 mmol) and 18-crown-6 (0.396 g, 1.5 mmol) in 10.0 mL of distilled water was stirred at room temperature for one hour and then filtered into a glass beaker for crystallization. The glass beaker was covered with a porous preservative film, and the filtrate was allowed to slowly evaporate at room temperature. After about 4-5 days, yellow-green block or prismatic crystals of

**DyFe18C6** suitable for X-ray analysis were obtained. The phase purity of their crystalline samples was checked by PXRD (Figure S2) and elemental analyses. Anal. Calcd for **DyFe18C6**: C, 29.66; H, 4.70; N, 11.53%. Found: C, 29.74; H, 4.61; N, 11.48%.

### 1.3 Orang samples for magnetic studies

Orang samples were obtained by illuminating the unirradiated samples at room temperature for 30 minutes by the laser. In order to avoid the orange sample recovering to yellow-green one, orange samples were then immediately sent to the tester for determination.

### 1.4 X-ray crystallographic study

Single-crystal X-ray diffraction measurement was performed on a Rigaku SCX mini diffractometer with Mo- $K_{\alpha}$  radiation ( $\lambda = 0.71073 \text{ \AA}$ ). There was no evidence of crystal decay during data collection, denoting the obtained compound was stable at ambient temperature. The intensity data sets were collected with the  $\omega$  scan technique and reduced by the CrystalClear software.<sup>1</sup> The primitive structure was solved by the direct method. The subsequent successive difference Fourier syntheses yielded the other non-hydrogen atoms. The final structure was refined using a full-matrix least-squares refinement on F<sup>2</sup>. All non-hydrogen atoms were refined anisotropically. Hydrogen atoms of 18-crown-6 molecule were added geometrically and refined using the riding model. Hydrogen atoms of all water molecules were located in the idealized positions and refined with O-H distances restrained to a target value of 0.85  $\text{\AA}$ , the H-H distance to 1.34  $\text{\AA}$ , and Uiso (H) = 1.5 Ueq (O). All calculations were performed by the Siemens SHELXTL version 5 package of crystallographic software.<sup>2</sup> The related crystal data and structure refinement results for **DyFe18C6** are given in Table S1. The selected bond distances and specified hydrogen bonds are given Tables S2 and S3, respectively.

The CCDC reference number for **DyFe18C6** is 1999915. Copy of the data can be obtained free of charge on application to CCDC, 12 Union Road, Cambridge CB2 1EZ, UK. [Fax: +44(1223)336-033; E-mail: [deposit@ccdc.cam.ac.uk.]

**References:**

1. *CrystalClear*, version 1.35; Software User's Guide for the Rigaku R-Axis, and Mercury and Jupiter CCD Automated X-ray Imaging System; Rigaku Molecular Structure Corporation: UT, **2002**.
2. *SHELXTL Reference Manual*, version 5; Siemens Energy & Automation Inc.: Madison, WI, **1994**.

## 2.Graphics.

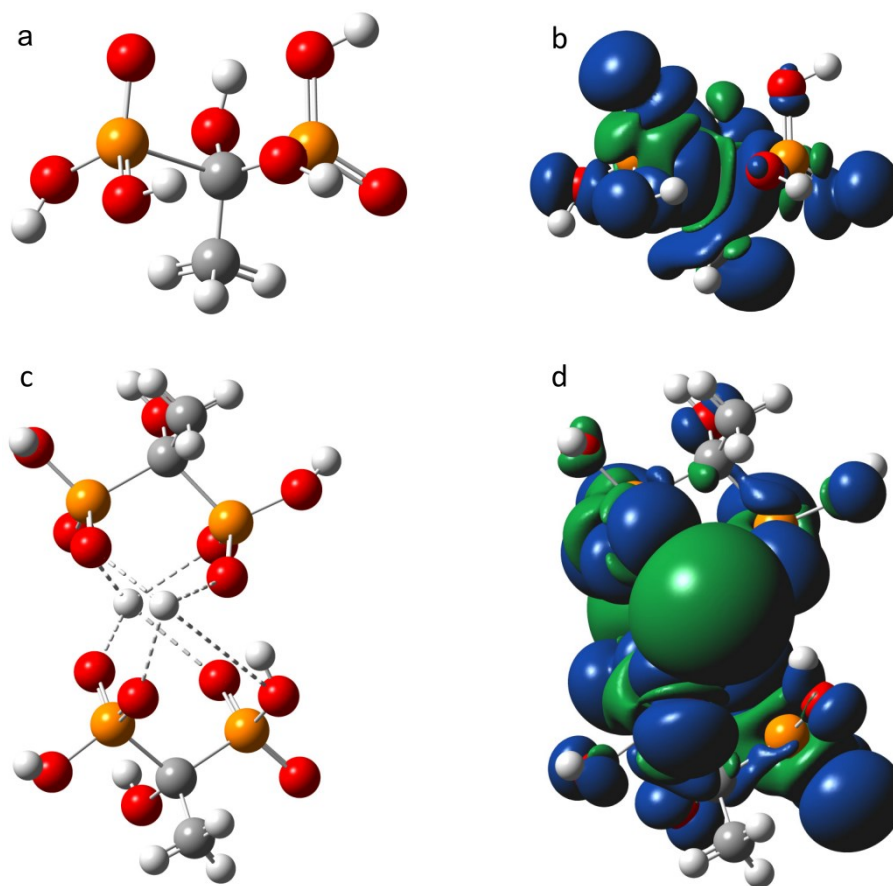


**Fig. S1.** Structures and spin density distributions of free HEDP (a,b; valence = +1, spin multiplicity = 2) and coordinated HEDP (c,d; valence = -1, spin multiplicity = 2) in **QDU-1(Dy)** supposing they lose one electron. Blue and green surfaces indicate  $\alpha$  and  $\beta$ -spin density distributions with 0.0004 au isosurfaces, respectively. The metal centers in the coordinated structure are replaced with H atoms. As can be seen, the spin delocalize to all O atoms instead of locating at the coordinated O atoms.

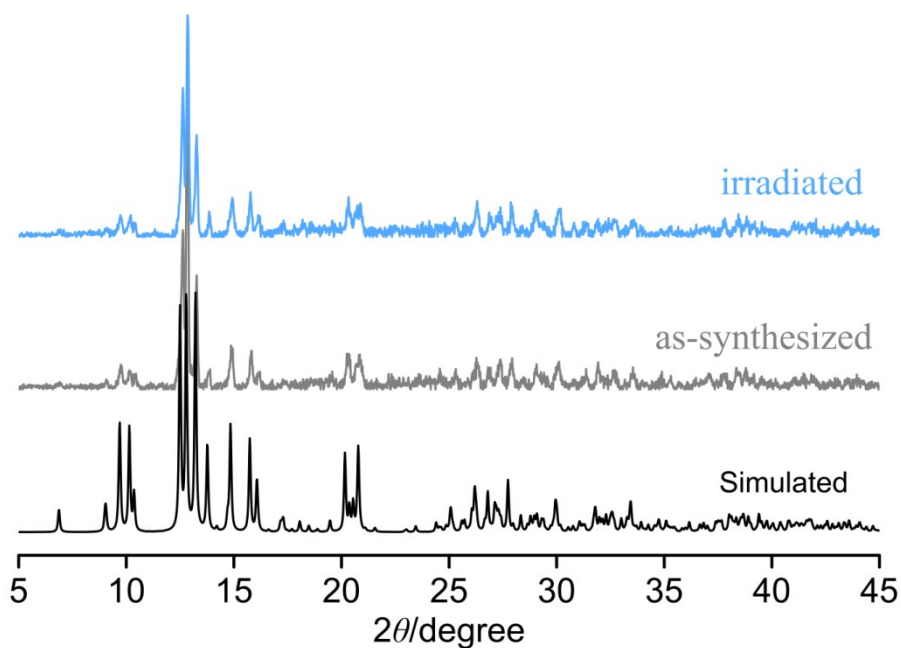


**Fig. S2.** PXRD patterns of **DyFe18C6** before and after irradiation. For comparison, the simulated data is also displayed.

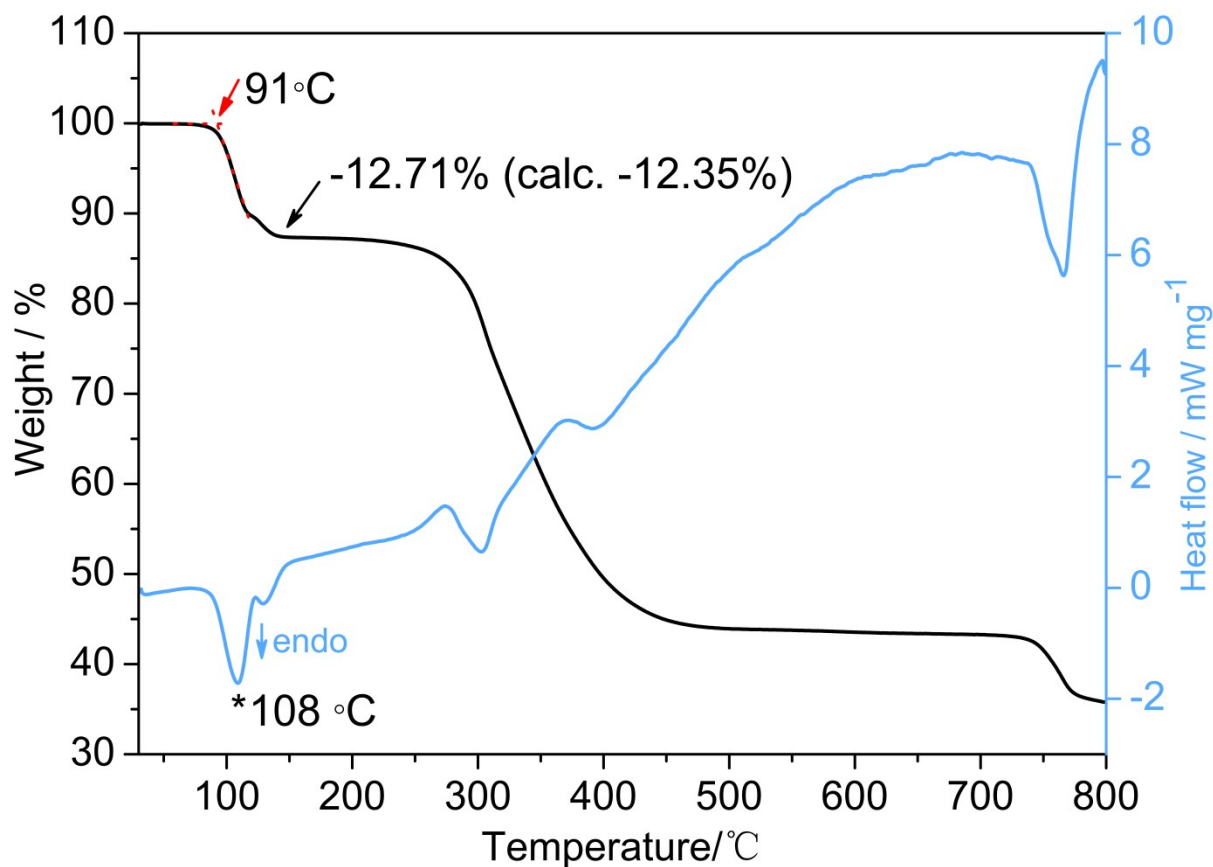


**Fig. S3.** TGA and DSC curves of as-synthesized **DyFe18C6**.

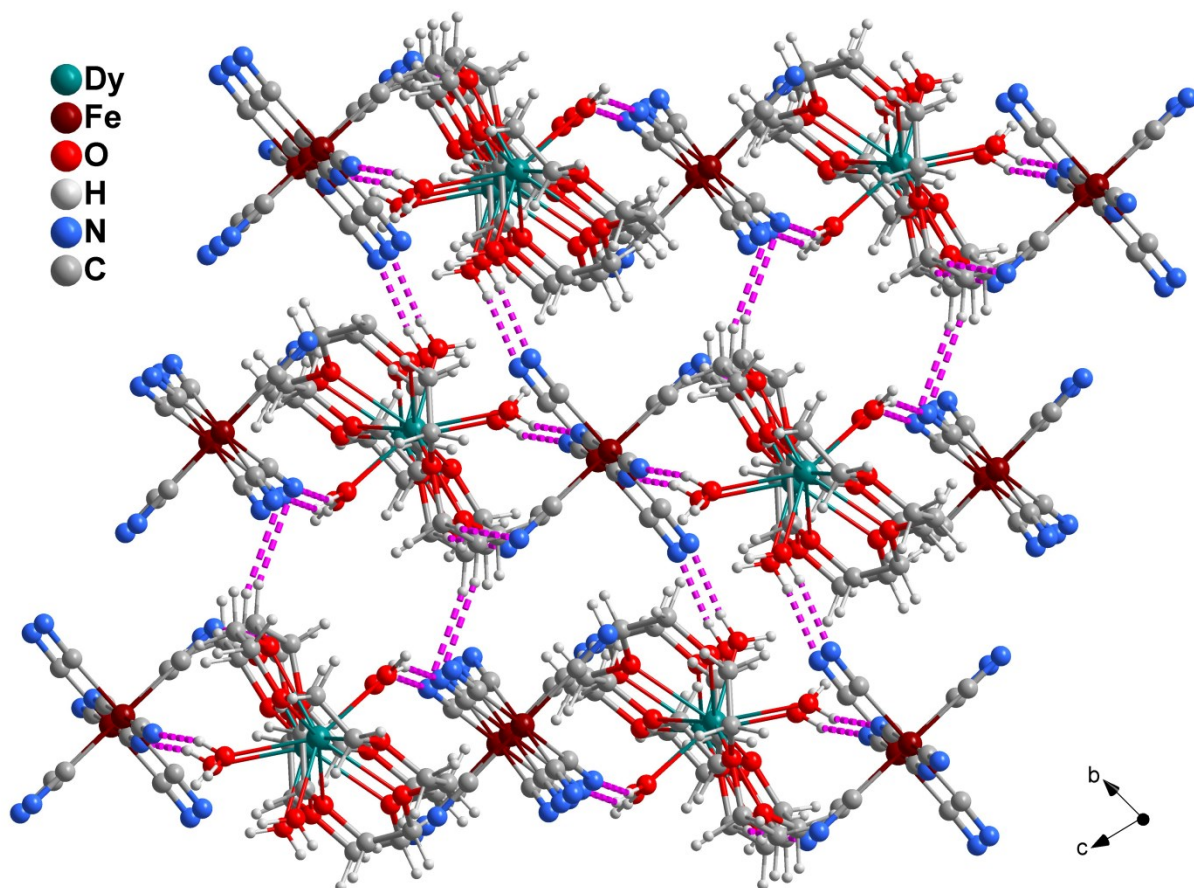


**Fig. S4.** 3D framework bridged by the hydrogen bonds of C–H···N and O–H···N

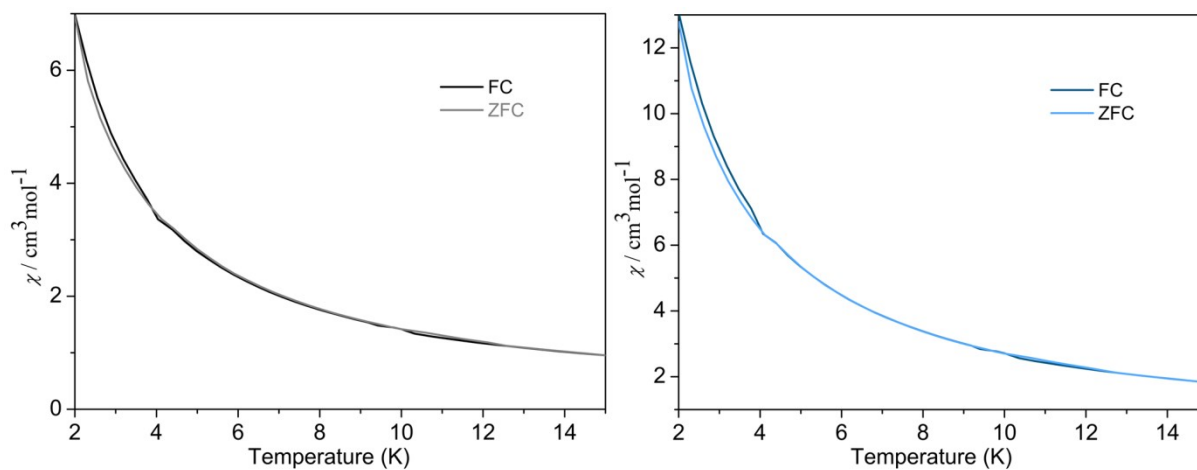


**Fig. S5.** Zero-field-cooled and 1000-Oe-cooled curves for **DyFe18C6** before (left) and after (right) irradiation.

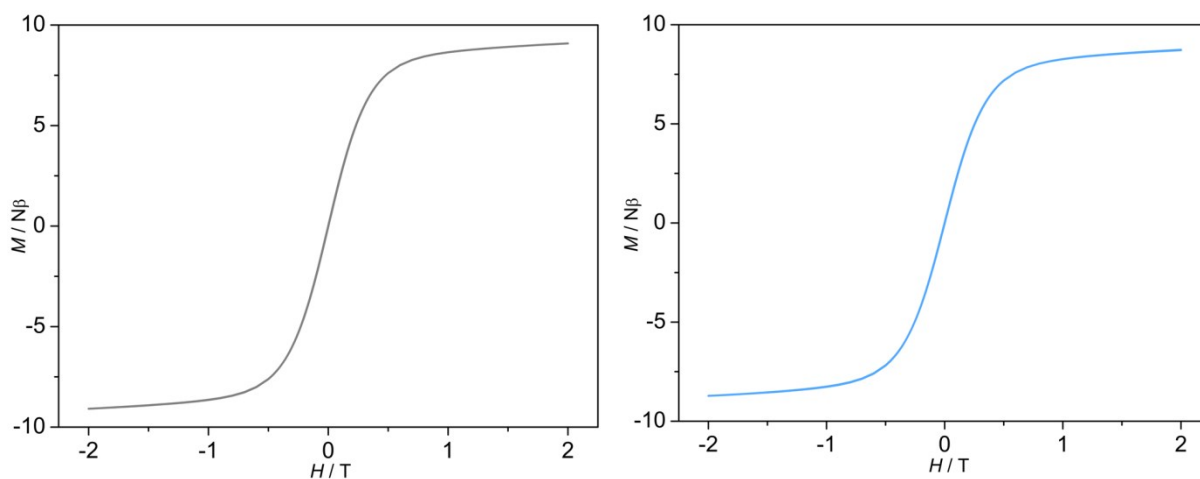


**Fig. S6.** Hysteresis loops at 2 K for **DyFe18C6** before (left) and after (right) irradiation.

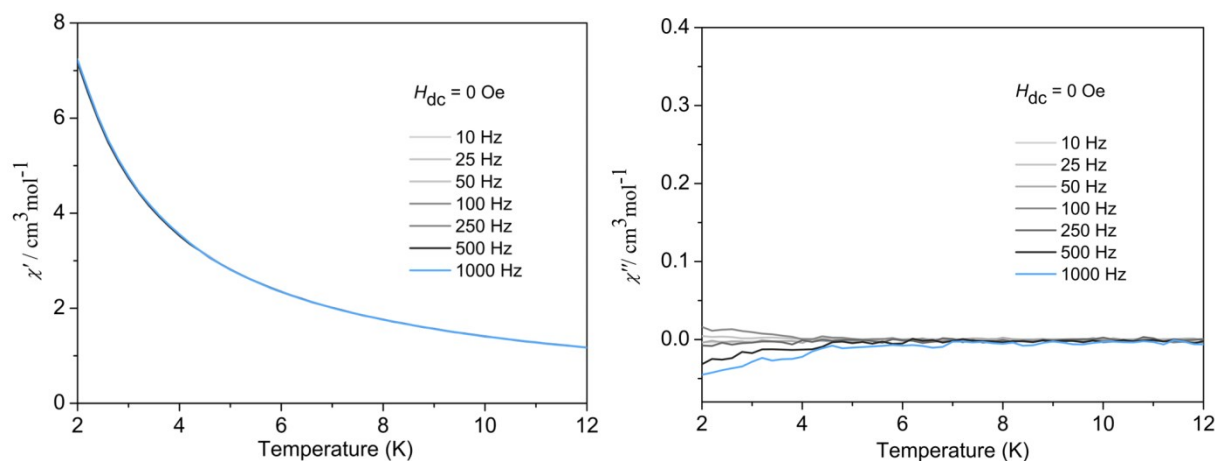


**Fig. S7.** Temperature-dependent in-phase (left) and out-phase (right) components of ac magnetic susceptibility for **DyFe18C6** before irradiation in a zero-dc field at various ac frequencies.

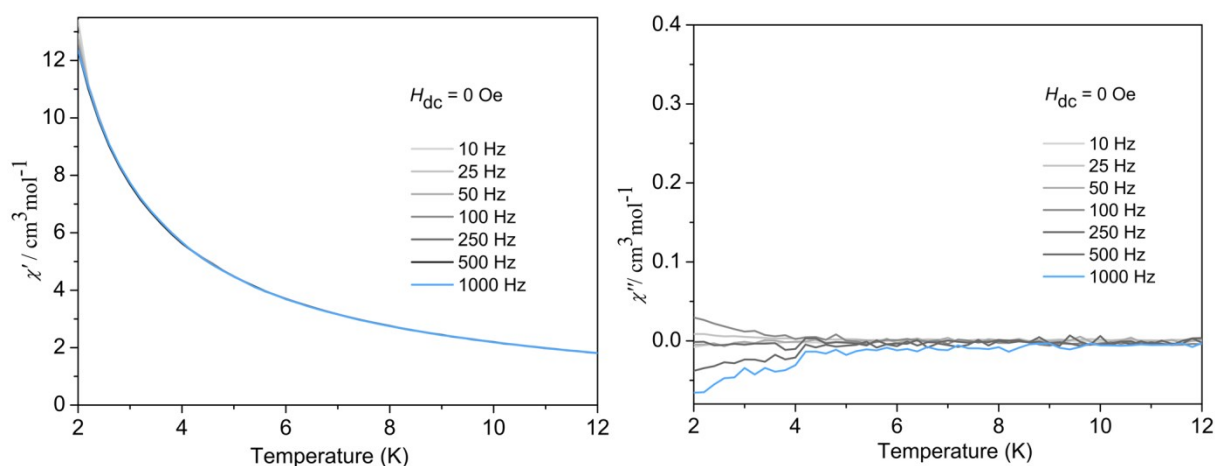


**Fig. S8.** Temperature-dependent in-phase (left) and out-phase (right) components of ac magnetic susceptibility for **DyFe18C6** after irradiation in a zero-dc field at various ac frequencies.



magnetic susceptibility for **DyFe18C6** after irradiation in a zero-dc field at various ac frequencies.

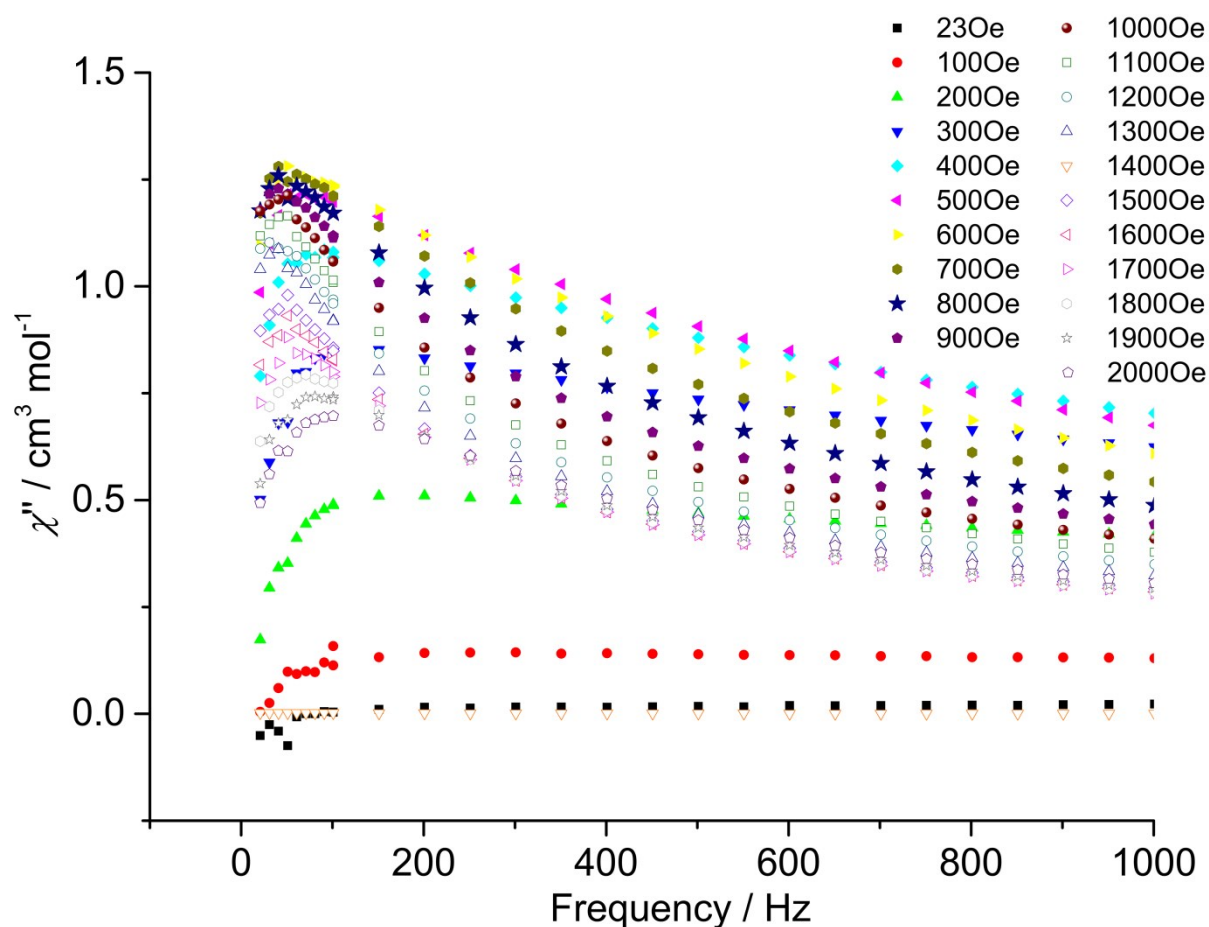


**Fig. 9.** Frequency-dependent out-phase components of ac magnetic susceptibility for **DyFe18C6** before irradiation in various dc fields.

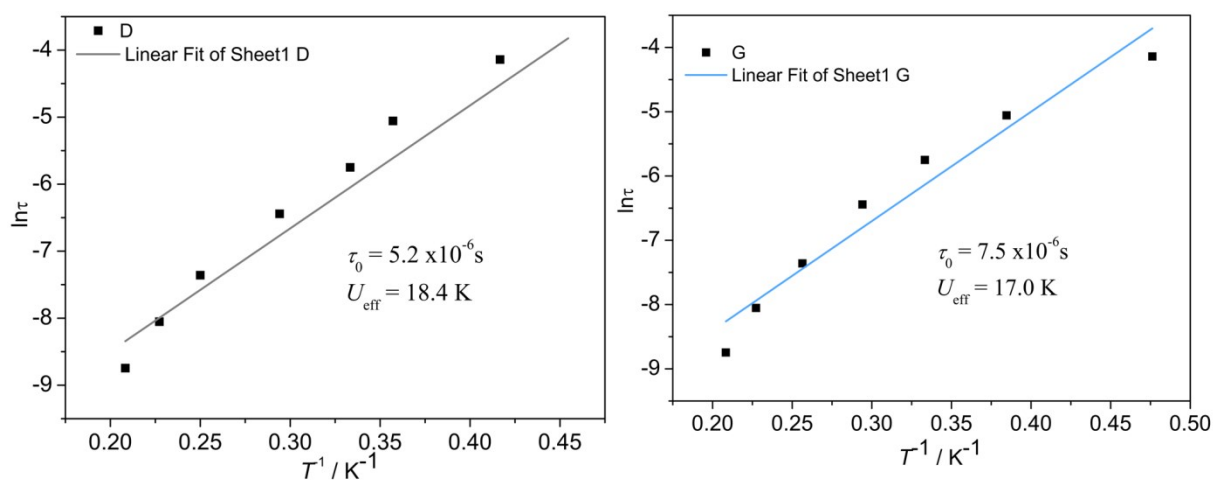


**Fig. S10.** Arrhenius plots for the magnetic relaxation process of **DyFe18C6** before (left) and

after (right) irradiation based on the peak values of  $\chi''$  in the temperature-dependent ac susceptibility data under an 800 Oe dc field. The full lines correspond to a linear fit.

### 3. Tables.

**Table S1.** Crystal data and structural refinements for as-synthesized **DyFe18C6** at 298 K.

Formula	$C_{18}H_{34}DyFeN_6O_{11}$
$M_r / \text{g mol}^{-1}$	728.86
Crystal system	Triclinic
Space group	$P\bar{1}$
$a / \text{\AA}$	11.029(3)
$b / \text{\AA}$	11.296(3)
$c / \text{\AA}$	14.213(4)
$\alpha / \text{deg}$	67.409(14)
$\beta / \text{deg}$	69.755(16)
$\gamma / \text{deg}$	64.550(15)
$V / \text{\AA}^3$	1441.0(7)
$Z$	2
$D_{\text{calcd}} / \text{g cm}^{-3}$	1.68
params/restraints/ data	367 / 17 / 5333
$F(000)$	728
GOF	1.020
$R_1^a [I > 2\sigma(I)]$	0.0320
$wR_2^b$ (all data)	0.0865

$$^a R_1 = \frac{\sum ||F_o| - |F_c||}{\sum |F_o|}; \quad ^b wR_2 = \left\{ \frac{\sum [w(F_o^2 - F_c^2)^2]}{\sum [w(F_o^2)^2]} \right\}^{1/2}.$$

**Table S2.** Selected bond lengths ( $\text{\AA}$ ) and angles ( $^\circ$ ) for as-synthesized **DyFe18C6**.

Dy1-O1	2.469(4)	O2W-Dy1-O3	76.43(15)
Dy1-O2	2.530(3)	O1W-Dy1-O3	133.15(14)
Dy1-O3	2.491(4)	O3W-Dy1-O3	76.09(14)
Dy1-O4	2.520(4)	O1-Dy1-O3	124.98(14)
Dy1-O5	2.473(3)	O5-Dy1-O3	106.23(15)

Dy1-O6	2.529(4)	O2W-Dy1-O4	106.32(14)
Dy1-O1W	2.350(3)	O1W-Dy1-O4	79.68(14)
Dy1-O2W	2.285(3)	O3W-Dy1-O4	80.84(15)
Dy1-O3W	2.352(3)	O1-Dy1-O4	155.67(16)
O2W-Dy1-O1W	144.69(14)	O5-Dy1-O4	62.99(14)
O2W-Dy1-O3W	144.09(13)	O3-Dy1-O4	62.89(14)
O1W-Dy1-O3W	70.76(12)	O2W-Dy1-O5	74.87(13)
O2W-Dy1-O1	98.01(15)	O1W-Dy1-O5	77.59(13)
O1W-Dy1-O1	80.37(14)	O3W-Dy1-O5	135.45(14)
O3W-Dy1-O1	79.53(15)	O1-Dy1-O5	125.33(14)
O2W-Dy1-O2	73.13(13)	O2W-Dy1-O6	75.38(14)
O1W-Dy1-O2	132.95(12)	O1W-Dy1-O6	72.55(14)
O3W-Dy1-O2	73.96(13)	O3W-Dy1-O6	130.92(13)
O1-Dy1-O2	63.28(12)	O1-Dy1-O6	63.06(14)
O5-Dy1-O2	147.82(13)	O5-Dy1-O6	62.73(14)
O3-Dy1-O2	62.83(13)	O3-Dy1-O6	151.59(14)
O4-Dy1-O2	123.98(14)	O4-Dy1-O6	122.79(14)
O6-Dy1-O2	111.39(14)		

**Table S3.** Geometries of the hydrogen bonds in as-synthesized **DyFe18C6**.

D-H...A	H...A/Å	D...A/Å	D-H...A/°
O1W-H1WB...N21	1.935	2.714	153.843
O5W-H5WB...N22	2.025	2.853	165.336
C9-H9A...N22	2.585	3.544	171.150
O3W-H3WB...N23	1.916	2.727	153.800
O4W-H4WA...N23	2.451	3.228	152.400
O4W-H4WB...N101	1.893	2.733	169.706
O5W-H5WA...N102	1.988	2.808	160.943
O2W-H2WB...N103	1.871	2.688	156.501
C10-H10A...N103	2.625	3.523	155.450

---

O3W-H3WB...O4W	1.885	2.714	163.768
O1W-H1WB... O4W	1.894	2.723	164.973
O2W-H2WB... O5W	1.756	2.615	172.225

---